Journal of Coordination Chemistry

ISSN: 0095-8972 (Print) 1029-0389 (Online) Journal homepage: https://www.tandfonline.com/loi/gcoo20

Structural and spectroscopic characterization of tetranuclear iron complexes containing a bridge

Michael Karnahl , Andreas Orthaber , Stefanie Tschierlei , Loganathan Nagarajan & Sascha Ott

To cite this article: Michael Karnahl , Andreas Orthaber , Stefanie Tschierlei , Loganathan Nagarajan & Sascha Ott (2012) Structural and spectroscopic characterization of tetranuclear iron complexes containing a bridge, Journal of Coordination Chemistry, 65:15, 2713-2723, DOI: 10.1080/00958972.2012.701008

To link to this article: https://doi.org/10.1080/00958972.2012.701008

Published online: 22 Jun 2012.

Journal of Coordination Chemistry
Vol. 65, No. 15, 10 August 2012, 2713–2723

Taylor & Francis
Taylor & Francis Group

Structural and spectroscopic characterization of tetranuclear iron complexes containing a $P_2^RN_2^{Ph}$ bridge

MICHAEL KARNAHL*†§, ANDREAS ORTHABER†§, STEFANIE TSCHIERLEI†, LOGANATHAN NAGARAJAN‡ and SASCHA OTT*†

†Department of Chemistry, Ångström Laboratory, Uppsala University, Box 523, 75120 Uppsala, Sweden
‡Department of Chemistry, Organic Chemistry, Lund University, Box 124, 22100 Lund, Sweden

(*Received 2 April 2012; in final form 30 May 2012*)

A pair of tetranuclear iron complexes consisting of two $Fe_2(Cl_2bdt)(CO)_5$ subunits (Cl_2bdt = 3,6-dicholorobenzene-1,2-dithiolate) bridged by different cyclic 1,5-diaza-3,7-diphosphacyclooctane (P_2N_2) ligands were prepared and structurally characterized. In the solid state, the P_2N_2 ligands adopt a boat conformation, which results in rather short distances between the two $Fe_2(Cl_2bdt)(CO)_5$ clusters that promotes electronic communication across the diphosphine ligand.

Keywords: Tetranuclear complexes; Iron carbonyl clusters; Hydrogenase models; X-ray crystallography; P_2N_2-ligands

1. Introduction

The development of efficient and sustainable proton reduction catalysts for hydrogen fuel generation is one of the largest challenges in the twenty-first century [1–4]. In this regard, nature gives inspiration for the design of catalysts for the reversible interconversion of protons to molecular hydrogen [5–9]. Particular enzymes, the so-called hydrogenases (H_2ases), are potential alternatives to rare and expensive noble metal catalysts [3, 10, 11] since they are based on earth abundant metals in their active sites [9, 12–15]. Depending on the number and the nature of transition metals, these enzymes are classified into [NiFe], [FeFe], and [Fe] H_2ases [12, 16–18]. While mononuclear [Fe] H_2ases exclusively oxidize H_2, dinuclear [FeFe] H_2ases also catalyze the reverse reaction, i.e. proton reduction. For this reason already more than 400 synthetic dinuclear model compounds have been prepared in attempts to mimic the [FeFe] H_2ase active site in structure and function [13, 15, 19–22]. The common feature

*Corresponding authors. Email: michael.karnahl@kemi.uu.se; sascha.ott@kemi.uu.se
§These authors contributed equally to this work.

Journal of Coordination Chemistry
ISSN 0095-8972 print/ISSN 1029-0389 online © 2012 Taylor & Francis
http://dx.doi.org/10.1080/00958972.2012.701008

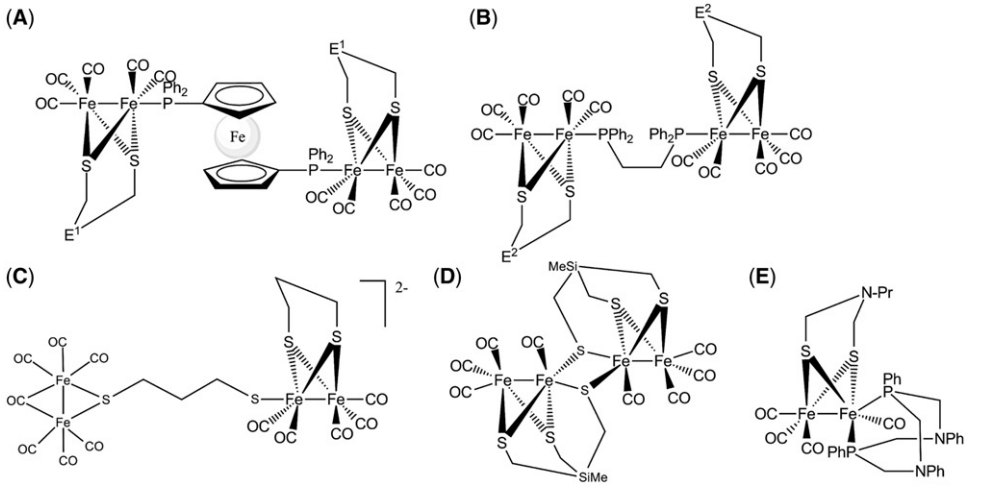

Figure 1. Overview of tetranuclear iron complexes **A–D** and the dinuclear complex **E**. (**A**) Ferrocenylbisphosphine (dppf) bridged diiron clusters, where $E^1 = CH_2$ [31] or O [32]. (**B**) Diphenylphosphinoethane (dppe) bridged Fe_2S_2 clusters, where $E^2 = CH_2$ or N–^{i}Pr [30] or CH-O-benzyl [33]. (**C**) Two Fe_2 units bridged by a propyldithiolate (pdt) moiety [35]. (**D**) Two Fe_2S_3 cores are connected *via* two κ^2 sulfur units [34]. (**E**) $P_2^{Ph}N_2^{Ph}$ acting as a bidentate ligand toward the same iron center [28].

of all of these model complexes is a Fe_2S_2 core with a wide range of different dithiolate bridges and various ligand combinations [13, 19, 20, 23]. Irrespective of this huge number of widely explored dinuclear models only very few tetranuclear iron complexes exist, which are the center of attention here.

Different approaches have been pursued to mimic enzymatic proton shuttle capabilities in the second coordination sphere, either *via* N (O) containing dithiolate bridges [19, 22–24] or *via* basic sites in phosphine ligands [5, 14, 25]. Especially insertion of such amine functionalities, acting as hydrogen/proton acceptors during the catalytic cycle, has become important.

Recently, the group of DuBois presented a series of mononuclear $[Ni(P_2^RN_2^{Ph})_2(CH_3CN)]^{2+}$ complexes with different substituents at the phosphorus atoms of the cyclic 1,5-diaza-3,7-diphosphacyclooctane (P_2N_2) ligand, which were used as electrocatalysts for hydrogen production [5, 26]. Moreover, DuBois *et al*. presented a $[Ni(diphosphine)_2]^{2+}$ catalyst with an extremely high turnover frequency for H_2 production exceeding 100,000 cycles per second [27]. Therefore, the use of such base-containing biphosphine (P_2N_2) ligands in combination with abundant Fe_2S_2 clusters turned out to be a promising approach [28, 29]. For instance, Lounissi *et al*. obtained a dinuclear Fe_2S_2 cluster in which the P_2N_2 acts as a bidentate ligand toward one iron (figure 1E) [28]. Although, several mono and dinuclear complexes of $P_2^RN_2^{R'}$ ligands are reported, tetranuclear iron complexes in which the P_2N_2 ligand acts as a bridging unit are unknown.

Upon abstraction/replacement of one CO, the remaining carbonyls experience a stronger back-bonding from the metal core which alters the reactivity of the complexes. Hence, formation of diiron clusters, in which only one CO has been replaced by one P of a bisphosphine ligand, leading toward tetranuclear assemblies, have been reported

earlier [30–33]. Figure 1 summarizes previously described tetranuclear iron complexes that contain bridging diphosphine (**A–B**) or disulfide units (**C–D**) [30–32, 34, 35].

2. Experimental

2.1. *Materials and methods*

If not stated otherwise, all reactions were carried out in an argon atmosphere using modified Schlenk techniques. Solvents were dried and distilled prior to use. Chemicals were obtained from Sigma-Aldrich, VWR, Fluka or ABCR and used as received.

The hexacarbonyl precursor [(Fe_2(μ-Cl_2bdt)$(CO)_6$] and the cyclic 1,5-diaza-3,7-diphosphacyclooctane ligands $P_2^RN_2^{Ph}$ with R = phenyl (Ph) or cyclohexyl (Cy) were prepared according to published procedures [36–40].

Nuclear magnetic resonance (NMR) spectra were recorded at ambient temperature on a JEOL Eclipse+ 400 and a Varian Mercury Plus 300 spectrometer operating at a proton frequency of 399.78 and 300.03 MHz, respectively. NMR spectra were referenced externally to tetramethylsilane or solvent residual peaks (^{1}H: $CDCl_3$ = 7.26 ppm, CD_3CN = 1.94 ppm). In the assignments, the chemical shift (δ in ppm) is given first, followed by the multiplicity of the signal in brackets and the number of protons (for ^{1}H-NMR).

Iron complexes are dissolved in freshly distilled CH_2Cl_2 at a final concentration of 1 mmol L^{-1}. IR absorption spectra were recorded in the spectral range of 4000–850 cm^{-1} with a resolution of 2 cm^{-1} on a Perkin Elmer SpectrumOne FTIR spectrometer. The IR measurements were performed with a liquid-sample-cell (Specac Omni-Cell) using CaF_2 windows with 0.5 mm PTFE spacers.

Electrochemical data were obtained by cyclic voltammetry using an Autolab potentiostat with a GPES electrochemical interface (Eco Chemie) and a standard three electrode setup. The working electrode was a glassy carbon disc (diameter 3 mm, freshly polished), while a glassy carbon stick was used as counter electrode. As reference electrode a non-aqueous Ag/Ag^+ electrode (CH Instruments, 10 mmol L^{-1} $AgNO_3$ in acetonitrile) with a potential of 80 mV (*vs.* the ferrocene/ferrocenium (Fc/Fc^+) couple) was used. Ferrocene was used as an internal standard and all reported potentials are quoted *versus* the Fc/Fc^+ couple. All measurements were conducted with oven dried glassware, freshly distilled dry CH_2Cl_2 and 0.1 mol L^{-1} tetrabutylammonium hexafluorophosphate $(Bu)_4NPF_6$ (Fluka, electrochemical grade) as supporting electrolyte.

2.2. *Preparation of the iron complexes*

2.2.1. [(Fe_2(μ-Cl_2bdt)$(CO)_5$)$_2$($P_2^{Ph}N_2^{Ph}$)] (1). The synthesis was carried out under argon in a Schlenk tube with freshly degassed acetonitrile (25 mL). In order to obtain the tetranuclear iron complex, the precursor [(Fe_2(μ-Cl_2bdt)$(CO)_6$] (150 mg, 0.31 mmol) was pretreated with $Me_3NO \cdot 2H_2O$ (37 mg, 0.33 mmol), resulting in a dark red solution. After 5 min, an excess of the 1,5-diaza-3,7-diphosphacyclooctane $P_2^{Ph}N_2^{Ph}$ (150 mg,

0.33 mmol) was added. The mixture was gently heated for 1 h at 60°C. The conversion was monitored by thin layer chromatography. The solvent was removed under reduced pressure and the solid residue was purified by chromatography on a silica gel column (CH_2Cl_2 : *n*-hexane, 1 : 1) yielding the dark red complex **1**. Yield: 52% (with respect to the iron precursor), $C_{50}H_{32}N_2P_2O_{10}S_4Cl_4Fe_4$ (1376.19 g mol^{-1}). Elemental analysis of a pristine sample shows no presence of dichloromethane, which might originate from the crystallization conditions. Anal. Calcd: C, 43.64; H, 2.34; N, 2.04; S, 9.32. Found: C, 43.53; H, 2.81; N, 1.92; S, 9.34. MS (ESI-nanospray in $CHCl_3$/$CH_3OH + CF_3COOAg$): m/z (%) = 1482.6 (100) $[M + Ag^+]^+$, 2860.2 (80) $[2M + Ag^+]^+$ with matching isotopic pattern. ^{1}H-NMR (400 MHz, $CDCl_3$): δ_H = 7.29–7.27 (m, 5H, CH_{arom}), 7.11–6.95 (m, 15H, CH_{arom}), 6.32 (s, 4H, Cl_2bdt), 4.79 (dd, $^2J_{HH}$ = 16, $^2J_{PH}$ = 2 Hz, 4H, CH_2), 4.32 ppm (dd, $^2J_{HH}$ = 16 Hz, $^2J_{PH}$ = 8 Hz, 4H, CH_2). ^{31}P{^{1}H}-NMR (161.8 MHz, $CDCl_3$): δ_P = 60.7 ppm. ^{13}C-NMR (75.5 MHz, $CDCl_3$): δ_C = 212.4 (s, CO), 212.3 (s, CO), 208.2 (br.s, CO), 152.6 (s), 150.1 (s), 137.7 (d, $^1J_{PC}$ = 33.9 Hz, P-C_{arom}), 132.0 (s), 129.9 (s), 129.8 (d, 9.0 Hz), 129.6 (s, C_{arom}H), 128.8 (d, 9.0 Hz), 128.4 (s, $C_{Cl\text{-}bdt}$H), 123.1 (s, para-C_{arom}H), 120.9 (s, C_{arom}H), 57.1 ppm (d, $^1J_{PC}$ = 18.1 Hz, CH_2). IR (CH_2Cl_2): ν_{CO} = 2057, 1998, and 1943 cm^{-1}.

2.2.2. [(Fe_2(μ-Cl_2bdt)(CO)$_5$)$_2$($P_2^{Cy}N_2^{Ph}$)] (2). Compound **2** was prepared as described for **1**, using 100 mg (0.205 mmol) [(Fe_2(μ-Cl_2bdt)(CO)$_6$] and 105 mg (0.225 mmol) of the cyclic $P_2^{Cy}N_2^{Ph}$ ligand, yielding the red **2**. Yield: 29% (with respect to the iron precursor), $C_{50}H_{44}N_2P_2O_{10}S_4Cl_4Fe_4$ (1388.29 g mol^{-1}). Anal. Calcd: C, 43.26; H, 3.19; N, 2.02. Found: C, 43.87; H, 3.26; N, 1.89. MS (ESI-nanospray in $CHCl_3$/$CH_3OH + CF_3COOAg$): m/z (%) = 1962.9 (100) $[M + Ag^+ + P_2^{Cy}N_2^{Ph}]^+$ with matching isotopic pattern. ^{1}H-NMR (400 MHz, $CDCl_3$): δ_H = 7.22 (m, 4H, CH_{arom}), 6.95 (m, 4H, CH_{arom}), 6.89 (m, 2H, para-CH_{arom}), 6.62 (s, 4H, Cl_2bdt), 4.45 (d, $^2J_{HH}$ = 16 Hz, 4H, CH_2), 4.35 (d, $^2J_{HH}$ = 16 Hz, 4H, CH_2), 2.06 (m, 2H, P-CH), 1.67 (m, 6H, CH_2), 1.53 (m, 4H, CH_2), 1.26 (m, 6H, CH_2), 1.11 ppm (m, 4H, CH_2). ^{31}P{^{1}H}-NMR (161.8 MHz, $CDCl_3$): δ_P = 69.2 ppm. ^{13}C-NMR (75.5 MHz, $CDCl_3$): δ_C = 212.7 (m, CO), 208.2 (m, CO), 206.7 (s, CO), 151.4 (s), 151.2 (s), 132.0 (s), 129.3 (s, C_{arom}H), 128.7 (s, $C_{Cl\text{-}bdt}$H), 121.3 (s, para-C_{arom}H), 117.9 (s, C_{arom}H), 54.3 (m, P-C-N), 37.0 (m, ipso-C_{cy}), 27.6 (br s, meta-C_{cy}), 26.7 (m, ortho-C_{cy}), 25.5 ppm (br s, para-C_{cy}). IR (CH_2Cl_2): ν_{CO} = 2056, 1996, and 1940 cm^{-1}.

2.3. *Crystallographic studies*

The crystal structure of **1** was determined on a Xcalibur (Oxford Diffraction) equipped with a Sapphire 3 CCD detector and a four-circle goniometer. The crystal structure of **2** was determined on a Bruker three-circle diffractometer equipped with an APEX II CCD detector. Experiments were conducted at 120 and 100 K for **1** and **2**, respectively (table 1). All measurements were conducted with Mo-Kα radiation using a graphite monochromator. Single crystals were mounted on a fiber loop and coated with N-paratone oil (Hampton Research). The structures were solved and refined using the SHELX suite of programs [41] using the WinGX software [42].

Table 1. Crystallographic data and refinement details for **1** and **2**.

Compound	**1**·CH_2Cl_2	**2**
Empirical formula	$C_{50}H_{32}Cl_4Fe_4N_2O_{10}P_2S_4 \cdot CH_2Cl_2$	$C_{50}H_{44}Cl_4Fe_4N_2O_{10}P_2S_4$
Formula weight	1461.08	1388.25
Crystal system	Monoclinic	Monoclinic
Space group	*C2/c* (No. 15)	$P2_1/c$ (No. 14)
Unit cell dimensions (Å, °)		
a	25.9569(14)	19.3330(10)
b	10.8194(4)	12.0435(6)
c	20.8007(8)	24.6295(12)
β	98.113(4)	98.802(3)
Volume (Å^3), *Z*	5783.2(4), 4	5667.1(5), 4
Calculated density (g cm^{-3})	1.677	1.627
Absorption coefficient (mm^{-1})	1.518	1.453
F(000)	2932	2816
Crystal size (mm^3)	$0.10 \times 0.10 \times 0.20$	$0.10 \times 0.10 \times 0.19$
Crystal description	Dark red plates	Red plates
Diffractometer	Oxford Xcalibur, Sapphire 3 CCD	Bruker Smart 3-circle, APEX II CCD
Temperature (K)	120(2)	100(2)
Wavelength (Å)	0.71073	0.71073
θ range for data collection (°)	2.7–27.0	1.7–26.6
Limiting indices	$-26 \le h \le 32$; $-13 \le k \le 13$; $-26 \le l \le 26$	$-24 \le h \le 21$; $-12 \le k \le 15$; $-30 \le l \le 30$
Reflections collected	18,851	43,397
Independent reflection	6256 [R(int) = 0.068]	11,697 [R(int) = 0.0653]
Parameters/restraints	357/0	685/0
S	0.97	1.102
Final *R* indices [$I > 2\sigma(I)$]	$R_1 = 0.0577$, $wR_2 = 0.1258$	$R_1 = 0.1166$, $wR_2 = 0.2894$
R indices (all data)	$R_1 = 0.1117$, $wR_2 = 0.1258$	$R_1 = 0.1399$, $wR_2 = 0.2894$
Largest difference peak and hole (e Å^{-3})	0.67 and −0.88	2.49 and −1.25

3. Results and discussion

Previous work describing the reactivity of bisphosphines toward Fe_2S_2 complexes reported a fine balance in either achieving the bridging tetranuclear or merely the dinuclear bidentate structural motif [30–32]. Very recently, it was reported that switching reaction conditions from boiling toluene to acetonitrile at 25°C changes the coordination of dppe from a chelating to a bridging mode [33]. In general, it is assumed that the reaction proceeds *via* a singly attached bisphosphine ligand, which can attack another iron center in an intermolecular fashion forming a bridged species, or through coordination to the same iron center resulting in a bidentate mode. Lounissi *et al*. [28]. stated that the cyclic bisphosphine $P_2^{Ph}N_2^{Ph}$ is very flexible and can act as a bidentate chelate toward one single iron center (figure 1, compound **E**). Accordingly, the dinuclear complex $[Fe_2(\mu\text{-pdt})(\kappa^2\text{-}P_2^{Ph}N_2^{Ph})(CO)_4]$ (pdt = 1,3-propyldithiolate) was prepared in refluxing toluene (18 h) and isolated in 49% yield from a product mixture [28]. Since it is known that pdt and bdt (1,2-benzyldithiolate) exhibit significantly different reactivity [43], we investigated the behavior of $[(Fe_2(\mu\text{-}Cl_2bdt)(CO)_6]$ toward P_2N_2 ligands.

3.1. *Synthesis and solid state structures*

The precursor complex $[(Fe_2(\mu\text{-}Cl_2bdt)(CO)_6]$ was prepared according to literature procedures [36, 43] and pretreated with $Me_3NO \cdot 2H_2O$ in order to facilitate

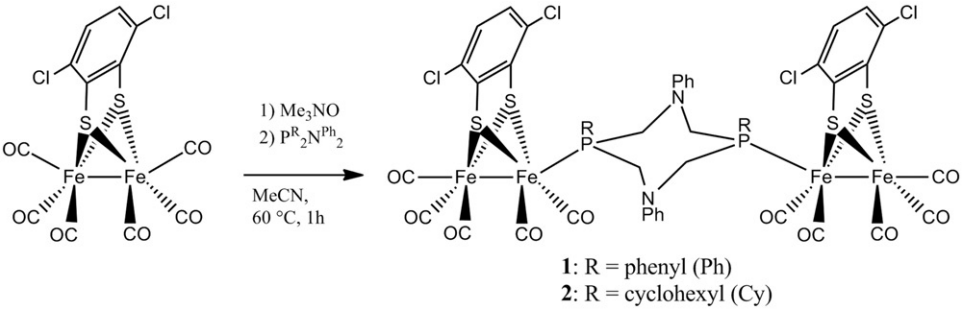

Scheme 1. Selective synthesis of the $P_2^RN_2^{Ph}$ bridged tetranuclear iron complexes **1** and **2**.

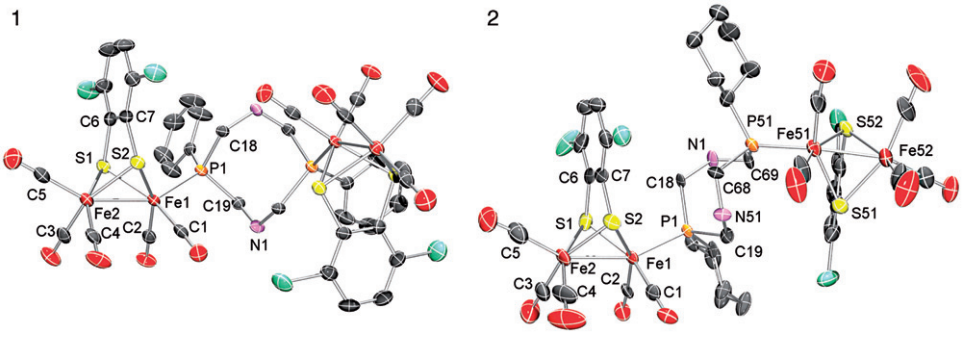

Figure 2. Molecular structure of **1** and **2** (ORTEP [45] with thermal ellipsoids at 50% probability level). Hydrogen atoms, phenyl substituents at the nitrogen, and co-crystallized solvent molecules are omitted for clarity.

replacement of one carbonyl [25]. Afterwards, an excess of the cyclic bisphosphine ligand $P_2^RN_2^{Ph}$ was added to the acetonitrile solution and kept at 60°C for 1 h (scheme 1). After chromatographic work up, **1** and **2** were obtained in 52% and 29% yield with respect to the dinuclear precursor, respectively. Hence, comparatively mild reaction conditions and short reaction times can be applied.

The full structural characterization of **1** and **2** was performed by NMR and IR spectroscopy, mass spectrometry (ESI-MS), and elemental analysis. Structural insights were obtained from X-ray crystallographic analysis of both **1** and **2** (figures 2 and 3, table 2). Single crystals of **1**, suitable for X-ray diffraction, were obtained by slow evaporation of a *n*-hexane/dichloromethane mixture. The $P_2^{Ph}N_2^{Ph}$ bridged bis(diiron) complex **1** crystallizes as dark red plates in the monoclinic space group *C2/c* as its dichloromethane solvate **1**·CH_2Cl_2. Single crystals of **2** were obtained by diffusion of pentane into dichloromethane under an inert atmosphere. Complex **2** crystallizes as red plates in the monoclinic space group $P2_1/c$. Further crystallographic details for structure solution and refinement can be found in the experimental section (table 1).

The solid state structures of **1** and **2** confirm the symmetric nature, in which the individual Fe_2S_2 cores exhibit similarity to the Fe_2S_2 unit in [(Fe_2(μ-Cl_2bdt)($CO)_6$]. Iron-sulfur distances (2.2722(15)–2.2815(14) Å for **1** and 2.255(3)–2.291(3) Å for **2**) are

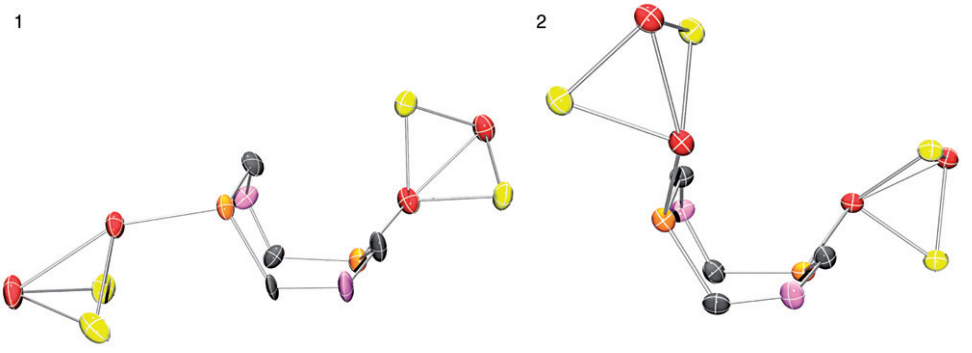

Figure 3. Structural details of **1** and **2** highlighting the coordination mode of the bridging $P_2^RN_2^{Ph}$ unit with respect to the Fe_2S_2 cores.

Table 2. Selected bond lengths (Å) and angles (°) for **1** and **2**.

	1	**2**
Fe1–Fe2 [Fe51–Fe52]	2.4788(10)	2.479(2) [2.470(2)]
Fe1–S1 [Fe51–S51]	2.2722(15)	2.287(3) [2.255(3)]
Fe1–S2 [Fe51–S52]	2.2815(14)	2.275(3) [2.272(3)]
Fe2–S1 [Fe52–S51]	2.2765(14)	2.285(3) [2.288(3)]
Fe2–S2 [Fe52–S52]	2.2765(14)	2.291(3) [2.274(3)]
Fe1–P1 [Fe51–P51]	2.2155(13)	2.236(2) [2.238(3)]
Fe1–C1 [Fe51–C51]	1.765(5)	1.741(12) [1.779(13)]
Fe2–C3 [Fe52–C53]	1.795(4)	1.783(15) [1.773(13)]
Fe2–C5 [Fe52–C55]	1.807(5)	1.794(15) [1.833(13)]
Fe2–Fe1–P1[Fe52–Fe51–P51]	150.96(5)	155.01(10) [154.21(10)]
Fe1–Fe2–C5 [Fe51–Fe52–C55]	152.46(15)	152.9(5) [150.3(4)]
Fe1–S1–Fe2 [Fe51–S51–Fe52]	66.04(4)	65.66(10) [65.85(9)]
Fe1–S2–Fe2 [Fe51–S52–Fe52]	65.92(4)	65.74(9) [65.81(9)]
C18–P1–C19 [C68–P51–C69]	111.2(2)	110.1(4) [110.2(4)]

in the normal range for this class of compounds [25, 36]. Furthermore, the Fe–Fe distances are 2.4788(10) Å for **1** and 2.479(2) [2.470(2)] Å for **2**, and hence very similar to the parent [$Fe_2(\mu$-$Cl_2bdt)(CO)_6$] complex (2.479(11) Å) [36]. This Fe–Fe distance is significantly shorter than in other tetranuclear complexes with dppe (2.5101(8) Å) [30, 31] or dppf bridges (2.5430(16)–2.5441(16) Å, figure 1) [32]. In contrast to the situation in **A** and **B** (figure 1), the P_2N_2 ligand can adopt different conformations. In the solid state, both bridging P_2N_2 ligands evince a boat conformation (figure 4), which is significantly widened in **2** as seen from the respective least squares planes (l. sq. pl.) spanned by the two P-C-N vertexes (**1**: 33.6(6)° and **2**: 72.6(11)°). Due to the different arrangement of the substituents at the phosphorus atoms, the two Fe_2S_2 subunits exhibit a rather short distance in **1** (Fe1–Fe1′: 6.741 Å), while it is as long as 7.447 Å for **2**. The Fe–P bond lengths are 2.2155(13) Å for **1** and 2.236(2) [2.238(3)] Å for **2** and hence on average slightly shorter than in other complexes with phosphine bridging ligands (2.2330(11)–2.265(2) Å) [30–33], but similar to related $P_2^{R1}N_2^{R2}$ complexes [28].

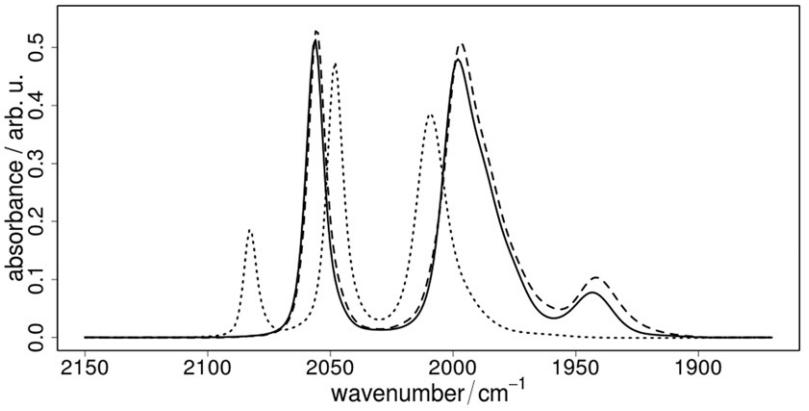

Figure 4. IR spectra of the carbonyl region of **1** (solid line), **2** (dashed line), and the parent complex [(Fe_2(μ-Cl_2bdt)($CO)_6$] (dotted line) dissolved in dichloromethane (1.0 mmol L^{-1}).

The Fe–P distances are hardly affected by coordination toward either one or two Fe_2S_2 cores, although the P-phenyl substituent in **1** results in marginally shorter Fe–P distances. Further structural details are given in table 2 and figure 3.

3.2. *Spectroscopic characterization of* 1 *and* 2

3.2.1. NMR spectroscopy. Both complexes exhibit only one ^{31}P-NMR signal at room temperature, which indicates a highly symmetric structure. The observed singlets at $\delta = 60.7$ ppm for **1** and $\delta = 69.2$ ppm for **2** are due to the different phosphorus substituents. A coordination shift $\Delta\delta_P$ ($\delta_{complex}$–δ_{ligand}) of 109.9 ppm for **1** ($P_2^{Ph}N_2^{Ph}$ ligand $\delta_P = -49.2$ ppm) and 108.6 ppm for **2** ($P_2^{Cy}N_2^{Ph}$ ligand $\delta_P = -39.4$ ppm) underlines the similarities between the two compounds. However, **2** is considerably less stable due to the easier oxidation of aliphatic phosphines compared to aromatic phosphines [44].

3.2.2. IR spectroscopy. Due to the strong absorption of carbonyls in an exclusive region, IR spectroscopy is a very sensitive tool to investigate ligand substitution reactions in iron carbonyl complexes [19, 38]. The hexacarbonyl precursor [(Fe_2(μ-Cl_2bdt)($CO)_6$] exhibits three intense $\nu_{C\equiv O}$ bands at 2082, 2048, and 2009 cm^{-1} (figure 4). Upon replacement of one carbonyl group and the introduction of the electron donating $P_2^RN_2^{Ph}$ bridging ligand to each Fe_2 subunit, the carbonyl bands of the tetranuclear complexes **1** and **2** experience a significant shift to lower wavenumbers (figure 4) [25, 46]. Hence, electron density at the iron centers is increased, resulting in a stronger backbonding into the CO antibonding orbitals. Interestingly, **1** and **2** are very similar in their respective vibrational C≡O frequencies, indicating only a marginal influence of the substituents R at the phosphorus (**1**: 2057, 1998, and 1943 cm^{-1}, **2**: 2056, 1996, and 1940 cm^{-1}). The difference between the $\nu_{C\equiv O}$ absorptions in **1** and **2** compared to those of **A** and **B** (figure 1) is presumably not due to the different bridge between the two Fe_2 subunits, but arises from the different dithiolate linkers in the individual Fe_2 sites.

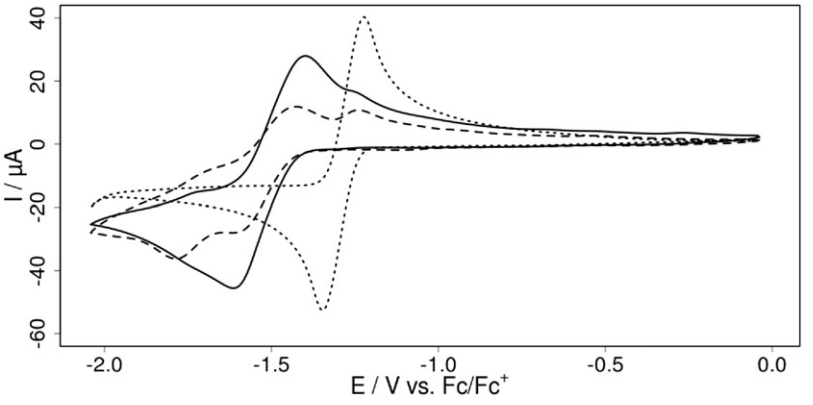

Figure 5. Cyclic voltammograms of **1** (solid line) and **2** (dashed line) in dichloromethane solution. The parent dinuclear complex (dotted line) is given for comparison and all potentials are referenced to the $Fc^{+/0}$ couple. Conditions: scan rate 100 mV s^{-1}, 0.1 mol L^{-1} $(Bu)_4NPF_6$ as supporting electrolyte, glassy carbon working electrode.

Complex **A** that contains pdt (E = CH_2): 2037, 1975, and 1926 cm^{-1} [31] or oxadithiolate (odt) ligands (E = O): 2047, 1983, and 1933 cm^{-1} [32] and **B** with pdt (E = CH_2): 2040, 1982, and 1922 cm^{-1} [30], substituted pdt (E = CH-O-benzyl): 2046, 1981, and 1933 cm^{-1} [33] or azadithiolate (adt) ligands (E = N-^{i}Pr): 2043, 1970, and 1936 cm^{-1} [30] (figure 1) all exhibit IR absorptions that are at lower energy compared to those of **1** and **2**. This finding is consistent with the weaker donor properties of bdt compared to that of aliphatic dithiolates [38].

3.2.3. Electrochemistry. Electrochemical behaviors of **1** and **2** were investigated by cyclic voltammetry. The reduction potentials of both tetranuclear complexes are more than 250 mV shifted toward negative potentials compared to that of [(Fe_2(μ-Cl_2bdt)$(CO)_6$] (figure 5), which is in agreement with significant red shifts in the IR spectra. The cyclic voltammogram of **2** exhibits two distinct reduction events at −1.60 and −1.78 V, which are in the characteristic region for [Fe^IFe^I]/[Fe^0Fe^I] reductions in conventional dinuclear [Fe_2S_2] complexes [19, 34, 36, 47]. Hence, the presence of two distinct anodic peaks may suggest an electronic coupling across the bisphosphine bridge between the two separated Fe_2S_2 cores. In contrast, **1** displays a broader reduction feature in dichloromethane solution, but still with a clear shoulder at a comparable potential.

4. Conclusions

We have demonstrated that P_2N_2 biphosphines can act as bridging ligands between two diiron dithiolate cores. The thereby obtained tetranuclear complexes **1** and **2** are selectively formed under relatively mild conditions, which contrasts the previously described complexes, where the P_2N_2 acts as a bidendate ligand to form **E** (figure 1).

Through different substituents at the phosphorus atoms a slight tuning of the electronic properties of the tetranuclear complexes can be achieved, although general geometric features remain unchanged. Phenyl substitution at phosphorus leads to a significantly improved stability of **1** compared to that of **2**. The cyclic voltammogram of **2** features two distinct reduction waves, suggesting a non-trivial electrochemistry.

Supplementary material

CCDC 874187 and 874188 contain the supplementary crystallographic data for **1** and **2**, respectively. These data can be obtained free of charge from The Cambridge Crystallographic Data Centre *via* www.ccdc.cam.ac.uk/data_request/cif

Acknowledgments

M.K. gratefully acknowledges the Wenner-Gren Foundation for a PostDoc fellowship. A.O. is grateful to the Austrian Science Fund (FWF) for an Erwin-Schrödinger fellowship (J 3193). S.T. thanks the German Academic Exchange Service (DAAD) and L.N. the Crafoord Foundation and Karl-Trygger Foundation for a postdoctoral fellowship. We also acknowledge the Knut and Alice Wallenberg Foundation for financial support and the X-ray diffractometer facility at Lund University, Sweden.

References

[1] A. Magnuson, M. Anderlund, O. Johansson, P. Lindblad, R. Lomoth, T. Polivka, S. Ott, K. Stensjö, S. Styring, V. Sundström, L. Hammarström. *Acc. Chem. Res.*, **42**, 1899 (2009).
[2] N. Armaroli, V. Balzani. *Angew. Chem. Int. Ed.*, **46**, 52 (2007).
[3] T.S. Teets, D.G. Nocera. *Chem. Commun.*, **47**, 9268 (2011).
[4] V. Balzani, A. Credi, M. Venturi. *ChemSusChem*, **1**, 26 (2008).
[5] M. Wang, L. Chen, L. Sun. *Energy Environ. Sci.*, **5**, 6763 (2012).
[6] P. Du, R. Eisenberg. *Energy Environ. Sci.*, **5**, 6012 (2012).
[7] M. Schulz, M. Karnahl, M. Schwalbe, J.G. Vos. *Coord. Chem. Rev.*, **256**, 1682 (2012).
[8] T.R. Cook, D.K. Dogutan, S.Y. Reece, Y. Surendranath, T.S. Teets, D.G. Nocera. *Chem. Rev.*, **110**, 6474 (2010).
[9] M.Y. Darensbourg. *Nature*, **433**, 589 (2005).
[10] S. Tschierlei, M. Karnahl, M. Presselt, B. Dietzek, J. Guthmuller, L. González, M. Schmitt, S. Rau, J. Popp. *Angew. Chem. Int. Ed.*, **49**, 3981 (2010).
[11] H. Ozawa, K. Sakai. *Chem. Commun.*, **47**, 2227 (2011).
[12] W. Lubitz, E.J. Reijerse, J. Messinger. *Energy Environ. Sci.*, **1**, 15 (2008).
[13] C. Tard, C.J. Pickett. *Chem. Rev.*, **109**, 2245 (2009).
[14] J.-F. Capon, F. Gloaguen, F.Y. Pétillon, P. Schollhammer, J. Talarmin. *Coord. Chem. Rev.*, **253**, 1476 (2009).
[15] M. Wang, L. Chen, X. Li, L. Sun. *Dalton Trans.*, **40**, 12793 (2011).
[16] J.W. Peters, W.N. Lanzilotta, B.J. Lemon, L.C. Seefeldt. *Science*, **282**, 1853 (1998).
[17] Y. Nicolet, C. Piras, P. Legrand, C.E. Hatchikian, J.C. Fontecilla-Camps. *Structure*, **7**, 13 (1999).
[18] F.A. Armstrong. *Curr. Opin. Chem. Biol.*, **8**, 133 (2004).
[19] S. Tschierlei, S. Ott, R. Lomoth. *Energy Environ. Sci.*, **4**, 2340 (2011).
[20] M.L. Singleton, N. Bhuvanesh, J.H. Reibenspies, M.Y. Darensbourg. *Angew. Chem. Int. Ed.*, **47**, 9492 (2008).

[21] M.K. Harb, U.-P. Apfel, J. Kübel, H. Görls, G.A.N. Felton, T. Sakamoto, D.H. Evans, R.S. Glass, D.L. Lichtenberger, M. El-khateeb, W. Weigand. *Organometallics*, **28**, 6666 (2009).
[22] J.M. Camara, T.B. Rauchfuss. *Nature Chem.*, **4**, 26 (2012).
[23] M.T. Olsen, T.B. Rauchfuss, S.R. Wilson. *J. Am. Chem. Soc.*, **132**, 17733 (2010).
[24] S. Ott, M. Kritikos, B. Åkermark, L. Sun, R. Lomoth. *Angew. Chem.*, **116**, 1024 (2004).
[25] S. Ezzaher, A. Gogoll, C. Bruhn, S. Ott. *Chem. Commun.*, **46**, 5775 (2010).
[26] U.J. Kilgore, M.P. Stewart, M.L. Helm, W.G. Dougherty, W.S. Kassel, M.R. DuBois, D.L. DuBois, R.M. Bullock. *Inorg. Chem.*, **50**, 10908 (2011).
[27] M.L. Helm, M.P. Stewart, R.M. Bullock, M.R. DuBois, D.L. DuBois. *Science*, **333**, 863 (2011).
[28] S. Lounissi, J.-F. Capon, F. Gloaguen, F. Matoussi, F.Y. Petillon, P. Schollhammer, J. Talarmin. *Chem. Commun.*, **47**, 878 (2011).
[29] M. Beyler, S. Ezzaher, M. Karnahl, M.-P. Santoni, R. Lomoth, S. Ott. *Chem. Commun.*, **47**, 11662 (2011).
[30] W. Gao, J. Ekström, J. Liu, C. Chen, L. Eriksson, L. Weng, B. Åkermark, L. Sun. *Inorg. Chem.*, **46**, 1981 (2007).
[31] X.-F. Liu, B.-S. Yin. *J. Coord. Chem.*, **63**, 4061 (2010).
[32] L.-C. Song, Z.-Y. Yang, H.-Z. Bian, Q.-M. Hu. *Organometallics*, **23**, 3082 (2004).
[33] L.-C. Song, W. Gao, X. Luo, Z.-X. Wang, X.-J. Sun, H.-B. Song. *Organometallics*, **31**, 3324 (2012).
[34] U.-P. Apfel, D. Troegel, Y. Halpin, S. Tschierlei, U. Uhlemann, H. Görls, M. Schmitt, J. Popp, P. Dunne, M. Venkatesan, M. Coey, M. Rudolph, J.G. Vos, R. Tacke, W. Weigand. *Inorg. Chem.*, **49**, 10117 (2010).
[35] I. Aguirre de Carcer, A. DiPasquale, A.L. Rheingold, D.M. Heinekey. *Inorg. Chem.*, **45**, 8000 (2006).
[36] L. Schwartz, P.S. Singh, L. Eriksson, R. Lomoth, S. Ott. *C. R. Chim.*, **11**, 875 (2008).
[37] G. Märkel, G. Yu Jin, C. Schoerner. *Tetrahedron Lett.*, **21**, 1409 (1980).
[38] L. Schwartz, L. Erikson, R. Lomoth, F. Teixisor, C. Vinas, S. Ott. *Dalton Trans.*, 2379 (2008).
[39] A.D. Wilson, R.H. Newell, M.J. McNevin, J.T. Muckerman, M. Rakowski DuBois, D.L. DuBois. *J. Am. Chem. Soc.*, **128**, 358 (2005).
[40] A.D. Wilson, K. Fraze, B. Twamley, S.M. Miller, D.L. DuBois, M. Rakowski DuBois. *J. Am. Chem. Soc.*, **130**, 1061 (2007).
[41] G. Sheldrick. *Acta Crystallogr. Sect. A: Found. Crystallogr.*, **A64**, 112 (2008).
[42] L.J. Farrugia. *J. Appl. Crystallogr.*, **32**, 837 (1999).
[43] D. Streich, M. Karnahl, Y. Astuti, C.W. Cady, L. Hammarström, R. Lomoth, S. Ott. *Eur. J. Inorg. Chem.*, 1106 (2011).
[44] T.E. Barder, S.L. Buchwald. *J. Am. Chem. Soc.*, **129**, 5096 (2007).
[45] L.J. Farrugia. *J. Appl. Crystallogr.*, **30**, 565 (1997).
[46] S. Ezzaher, J.-F. Capon, F. Gloaguen, F.Y. Pétillon, P. Schollhammer, J. Talarmin, R. Pichon, N. Kervarec. *Inorg. Chem.*, **46**, 3426 (2007).
[47] G.A.N. Felton, C.A. Mebi, B.J. Petro, A.K. Vannucci, D.H. Evans, R.S. Glass, D.L. Lichtenberger. *J. Organomet. Chem.*, **694**, 2681 (2009).